ACS APPLIED ENERGY MATERIALS
Cite This: ACS Appl. Energy Mater. 2018, 1, 4453−4458
Letter
www.acsaem.org

Sulfur-Rich MoS_6 as an Electrocatalyst for the Hydrogen Evolution Reaction

Oluwaniyi Mabayoje,[†] Bryan R. Wygant,[†] Michael Wang,[‡] Yang Liu,[‡,§] and C. Buddie Mullins*[,†,‡,∥]

[†]Department of Chemistry, University of Texas at Austin, Austin, Texas 78712, United States
[‡]Department of Chemical Engineering, University of Texas at Austin, Austin, Texas 78712, United States
[§]College of Chemistry and Chemical Engineering, Central South University, Changsha 410083, China
[∥]Texas Materials Institute, University of Texas at Austin, Austin, Texas 78712, United States

Supporting Information

ABSTRACT: In this work, we studied a sulfur-rich molybdenum sulfide (MoS_6) hydrogen evolution reaction (HER) catalyst prepared by chemical oxidation of thiodimolybdate ($Mo_2S_{12}^{2-}$). Using X-ray photoelectron spectroscopy, X-ray diffraction, and other techniques, we found that the material had an overall S:Mo ratio of 6:1 and is likely an amorphous coordination polymer of molybdenum−sulfur (Mo_3-like) clusters with the additional sulfur existing as bridging or terminal disulfide moieties. Used as a HER catalyst, MoS_6 has an HER overpotential of 130 mV at 10 mA/cm^2, compared to 178 mV for MoS_4 samples made from tetrathiomolybdate (MoS_4^{2-}). Electrochemical surface area measurements show that the improved performance of MoS_6 over MoS_4 was not due to the sulfur-rich material having a higher surface area. Instead, we ascribe the performance of the sulfur-rich MoS_6 catalyst to the presence of additional disulfide active sites compared to other amorphous MoS_x catalysts. This study highlights the possibility of using different thiomolybdate precursors to synthesize novel MoS_x HER catalysts.

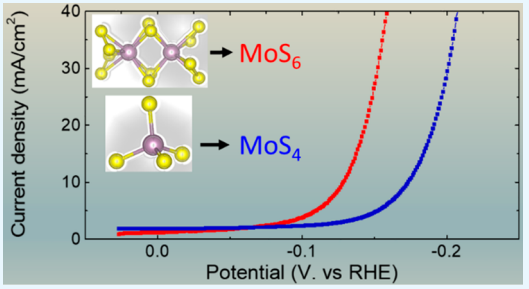

KEYWORDS: *hydrogen evolution, electrocatalysis, molybdenum sulfide, energy conversion, solar water splitting*

The hydrogen evolution reaction (HER), $2H^+ + 2e^- \rightarrow H_2$, is an important reaction in the electrochemical production of hydrogen as a chemical fuel.[1,2] Beyond its possible application to reducing some of the energy and environmental issues facing the world, this reaction is also important because of its apparent simplicity; it involves only two protons in solution combining with two electrons to produce hydrogen gas. Thus, understanding this reaction is a starting point that will enable electrochemists to begin developing a very fundamental understanding of active sites and substrate adsorption in inner sphere heterogeneous electrode reactions.[3]

Traditional catalysts used for the HER include expensive noble metals or alloys of noble metals like Pt and Pd.[4] Initially, crystalline molybdenum sulfide (MoS_2) was investigated as an electrocatalyst for the HER and found to be relatively effective compared to other inexpensive non-noble metal-based catalysts, achieving overpotentials of 300−400 mV for 10 mA/cm^2.[5−7] Further work focused on nanostructuring and increasing the density of active sites by exfoliating the MoS_2 sheets and increasing the density of exposed active edge sites.[8] While crystalline molybdenum sulfide showed promise, Hu et al. later demonstrated that amorphous MoS_x catalysts were even more active for the HER than the crystalline MoS_x catalysts.[9−12] Furthermore, amorphous catalysts usually required comparably milder conditions for their synthesis than did crystalline MoS_2 catalysts. They are typically prepared by either the electrochemical deposition of thin films[9] or by wet chemical synthesis,[11] without the need for high temperatures. The simple synthesis of these amorphous catalysts and the ability to produce them in large quantities make them promising HER catalysts.[11,13,14]

An additional motivation for studying amorphous molybdenum sulfide catalysts is the ability to modify properties like the Mo/S ratio and structure due to the richness of molybdenum−sulfur chemistry.[15] Amorphous molybdenum sulfide (a-MoS_x) catalysts have been shown to be composed of inorganic polymeric structures.[14] It is expected that the monomeric units in these polymers control the catalytic properties of these materials. The relatively low temperatures needed to make these materials is also significant, as it suggests control of stoichiometry and structure while minimizing changes in the morphology of the materials due to sintering.

In this paper, we report the use of sulfur-rich MoS_6 as an HER catalyst. We show that this material, with a higher sulfur content than the often studied MoS_4 catalyst, can be obtained by changing the precursor from the commercially available

Received: June 14, 2018
Accepted: September 10, 2018
Published: September 10, 2018

DOI: 10.1021/acsaem.8b00973
ACS Appl. Energy Mater. 2018, 1, 4453−4458

tetrathiomolybdate (MoS_4^{2-}) anion to the more exotic thiodimolybdate ($Mo_2S_{12}^{2-}$) anion.

$$(NH_4)_2Mo_2S_{12} + I_2 \rightarrow 2NH_4I + 2MoS_6 \quad (1)$$

Sulfur-rich molybdenum sulfide particles were prepared by oxidizing $Mo_2S_{12}^{2-}$ with chemical oxidants like I_2 (or $S_2O_8^{2-}$, as described in the Supporting Information) at room temperature in dimethylformamide (DMF). This, we anticipate, will be a first step toward controlling the stoichiometry, structure, and activity of MoS_x HER catalysts while obtaining important structure−activity correlations that could help in developing a better understanding of the HER and the electrocatalysts that perform it.

A transmission electron microscopy (TEM) image (Figure 1a) shows a representative as-synthesized MoS_6 particle. The

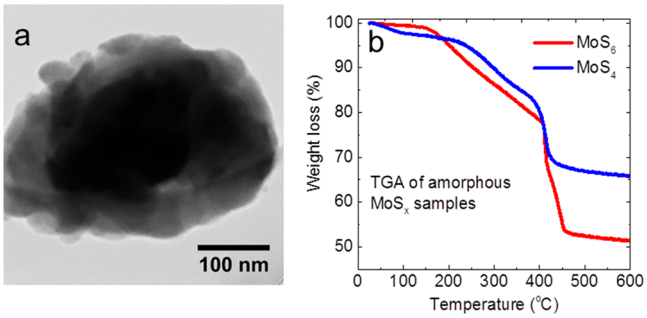

Figure 1. (a) Transmission electron micrograph of a representative MoS_6 particle. (b) Thermogravimetric analysis showing the mass loss of MoS_x samples as they are heated to 600 °C at a ramp rate of 10 °C/min in argon. MoS_6 (red curve) loses more of its initial mass compared to MoS_4 (blue curve).

average particle size is fairly large, with most particles falling in the 400−800 nm diameter range. In agreement with past studies on molybdenum sulfides synthesized from molybdate precursors at room temperature, selected area diffraction patterns (SAED) showed only diffuse rings indicating an absence of long-range order in this material (Figure S1).[16] Scanning electron microscopy images (Figure S2) suggest that the particles seen in TEM images agglomerate into larger structures.

Next, we measured the bulk molybdenum−to-sulfur ratio in the material by thermogravimetric analysis (TGA, Figure 1b). The sulfur content can be measured by this means because amorphous MoS_x samples are known to convert to crystalline MoS_2 at high temperatures under inert atmosphere.[15,16] Gradual weight loss before 200 °C represents the loss of residual solvent. The molybdenum sulfides decompose in multiple stages from 200 to 460 °C.

$$MoS_{2+x} \rightarrow MoS_2 + xS \quad (2)$$

From the above eq 2, a sample with a S/Mo ratio of 6 would lose about 44% of its mass as the sulfur decomposes and the material is converted to MoS_2 at high temperatures (details in the Supporting Information). We found that the samples prepared by oxidizing the $Mo_2S_{12}^{2-}$ with I_2 lost 44.4% of their mass during the TGA, in agreement with a S/Mo ratio of 6. A comparison of this sulfur-rich sample with the control MoS_x sample made by similarly oxidizing MoS_4^{2-} shows the control samples only lose 29% of their initial mass, in agreement with an expected S/Mo ratio of 4. The TGA plot shows that the samples made by using the thiodimolybdate precursor are relatively sulfur-rich in the bulk when compared to samples made using the tetrathiomolybdate anion.

Sulfur-rich MoS_6 samples were further studied using X-ray photolelectron spectroscopy (XPS) as shown in Figure 2 (a

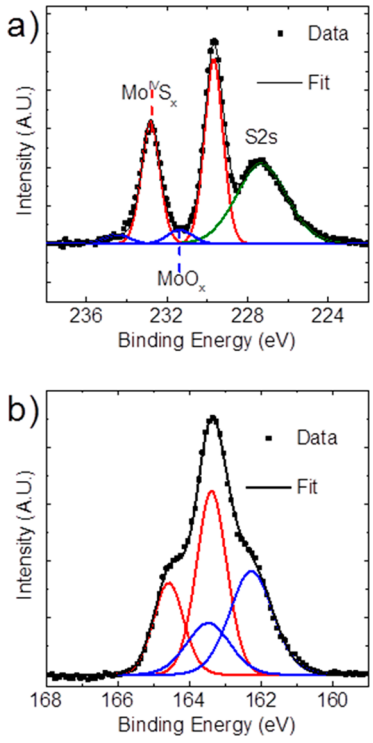

Figure 2. XPS spectra for sulfur-rich MoS_6 particles. The Mo 3d region shows the presence of Mo^{IV} sulfides, MoO_x defects, and the overlapping S 2s region (a). The S 2p region shows the presence of four peaks (two doublets associated with polysulfides) (b).

survey spectrum is shown in Figure S3). The molybdenum 3d region shows a doublet at 229.6 and 232.7 eV assigned to Mo^{IV} sulfides. Additionally, we see peaks showing some molybdenum oxide species on the surface of this material.[14] These Mo peaks overlap with the S 2s region; to observe the molybdenum peaks without the overlapping sulfur region, we also took measurements of the Mo 3p region (Figure S4). The sulfur 2p region was deconvoluted and analyzed (Figure 2b); four peaks (two doublets) can be seen in this region. The first peaks at higher binding energy (at 163.4 and 164.6 eV) correspond to bridging (S_2^{2-}) and apical (S^{2-}) sulfur groups while the second set of peaks (at 162.3 and 163.5 eV) belongs to terminal (S_2^{2-}) and shared (S^{2-}) groups.[13,14,18,19] The first set of doublets at higher binding energies make up 58.5% of the sulfur atoms while the second set of peaks make up the remaining 41.5%. The presence of all these peaks is generally associated with molybdenum polysulfides.[14] The lack of a clear peak attributable to elemental sulfur in this region (typically seen at higher binding energies than the sulfides) indicates that most of the sulfur in our material is bonded with molybdenum. This is also consistent with the fact that our samples were washed with CS_2 which is known to dissolve sulfur impurities. We examined the Mo:S ratio of this sample to verify that the surface ratio was consistent with the bulk stoichiometry obtained by thermogravimetric analysis. Integration of the peaks in the Mo 3d region and the S 2p peaks gives a Mo:S

DOI: 10.1021/acsaem.8b00973
ACS Appl. Energy Mater. 2018, 1, 4453−4458

ratio of 1:5.9 in agreement with the bulk ratio determined by TGA.

Next, we attempted to characterize the material's structure by XRD (Figure 3a) and found that the diffractogram lacked

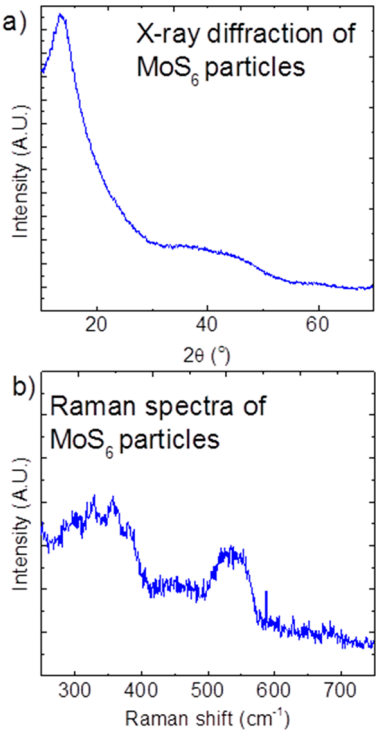

Figure 3. (a) X-ray diffraction and (b) Raman spectra for sulfur-rich MoS_6 particles.

sharp peaks and was dominated by broad features which indicate the material is amorphous, in agreement with both our SAED results (Figure S1) and with past results.[16] This is in contrast to the sharp peaks observed in the diffractogram of the $Mo_2S_{12}^{2-}$ precursor (Figure S5). Studies have shown that molybdenum sulfides synthesized at room temperature lack long-range crystalline order but have short-range atomic order.[11,14] The features observed in the Raman measurements (Figure 3b) at low laser power are similarly broad. The absence of well-defined peaks, as mentioned earlier, is indicative of the short-range atomic arrangement in this material. The centers of these broad peaks are consistent with Raman measurements of amorphous molybdenum sulfides (MoS_3) which are known to be inorganic coordination polymers of Mo_3S_{13} clusters.[18] Despite the broadness of these peaks, certain features can be identified.[17] We assign the features between 280 and 400 cm^{-1} to the Mo−S stretching frequencies as previously reported, and the broad peak between 500 and 550 cm^{-1} is associated with the S−S stretching frequencies typical of materials with polysulfides.[14,18] The presence of these peaks in our samples suggests that these sulfur-rich MoS_6 particles are similarly made up of Mo_3S_{13}-like clusters. As previously reported in the literature, measurements at higher laser power converted the material into a mixture of MoS_2 and MoO_3 over the course of a few seconds (Figure S6).[20]

Maintaining a molybdenum oxidation state of +4 while incorporating a relatively high amount of sulfur in a nonelemental state indicates that the sulfur-rich MoS_6 must include more terminal or/and bridging S_2^{2-} sulfur species compared to the MoS_4 samples.[17] A similar analysis comparing two amorphous ReS_x samples with slightly different S/Re ratios (ReS_4 and Re_2S_7) concluded that the sample with the higher sulfur-to-rhenium ratio (Re_2S_7) had more disulfide bonds existing as bridging sulfur moieties.[21] Returning to the molybdenum sulfide samples of the present study, on the basis of the XPS results taken together with the XRD and Raman spectroscopy results, we propose that this MoS_6 catalyst is also an amorphous coordination polymer of molybdenum−sulfur (Mo_3-type) clusters (Figure 4a) that incorporate the excess sulfur as bridging or/and terminal sulfide moieties.[17] Reasonable structures can be proposed on the basis of the studies of ReS_x materials mentioned above. The excess sulfur can be incorporated either as bridging disulfide moieties (Figure 4b) or as terminal sulfide moieties (Figure 4c). Hibble et al. have shown using a combination of in situ infrared spectroscopy and extended X-ray absorption fine structure (EXAFS) that $(NH_4)_2Mo_2S_{12}$ samples annealed at low temperatures go through a major structural change from Mo_2 clusters to Mo_3S_{13}-like clusters while retaining additional sulfur atoms as terminal sulfides which become shared sulfur moieties in the coordination polymer. For this reason, we believe our samples incorporate the additional sulfur atoms as shared sulfide moieties.[22] While the exact nature of the active sites in MoS_x catalysts is yet to be determined, it is accepted that sulfur functionalities influence the HER activity of MoS_x catalysts.[6,23] Using a combination of XPS and Raman spectroscopy, Ting et al. have shown that the terminal and bridging sulfur moieties are the true active sites for the HER.[18]

Next, we examined the activity of the sulfur-rich MoS_x samples as HER catalysts in an electrochemical cell with 0.5 M H_2SO_4 as the electrolyte. Dissolved oxygen was removed from

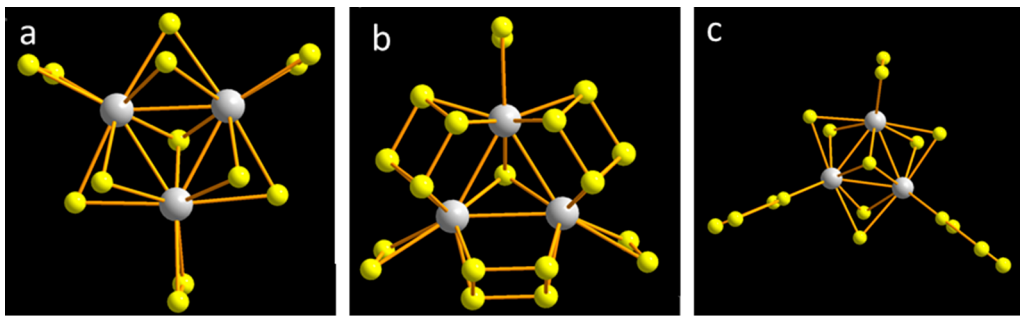

Figure 4. (a) Mo_3S_{13} clusters are known components of amorphous MoS_x catalysts. Proposed structures for Mo_3 clusters in sulfur-rich MoS_6 catalysts with additional sulfur bonds as (b) bridging and (c) shared sulfide moieties.

DOI: 10.1021/acsaem.8b00973
ACS Appl. Energy Mater. 2018, 1, 4453−4458

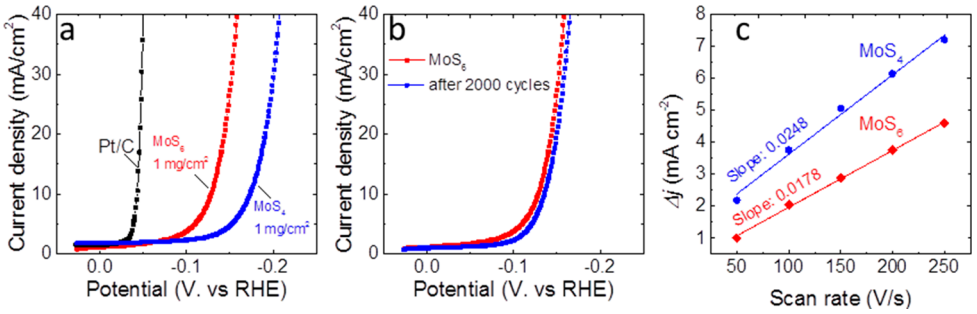

Figure 5. (a) Linear sweep voltammetry (LSV) voltamograms of MoS_6 (red curve) and MoS_4 (blue curve) samples (mass loadings of and 1 mg/cm^2) and a benchmark Pt/C catalysts for the hydrogen evolution reaction (HER). (b) LSV curves showing the initial polarization curve and a polarization curve after 2000 (scan rate: 50 mV/S) cyclic voltammetry (CV) cycles. (c) Scan-rate dependent current density at 0.5 V vs Ag/AgCl for MoS_4/VC samples (blue line) and MoS_6/VC (red line) samples. The scan rate for parts a and b is 10 mV/s.

the electrolyte by purging with Ar for 40 min before electrochemical testing and during tests. Experiments were carried out by first running a cyclic voltammetry experiment (20 cycles between 0.1 and −0.35 V vs RHE at a scan rate of 100 mV/s) on samples mixed with Vulcan carbon and deposited on a glassy carbon electrode (Figure S7). The first polarization curve shows cathodic peaks and a later onset of the currents for the hydrogen evolution reaction. Subsequent cycles showed earlier onsets of the catalytic currents for the HER (10 mA/cm^2 of current at 210 mV for the first cycle vs at ∼165 mV for subsequent cycles). The activation of MoS_x HER catalysts following reductive cycling has previously been seen by other researchers. Benck and co-workers used XPS to study the activation of these catalysts in acidic electrolytes and observed a significant decrease in the intensity of peaks previously attributed to surface molybdenum oxide (MoO_x) species.[13] Tran and co-workers also used Raman spectroscopy and CV experiments in electrolytes at different pH values to show that the catalytic peaks observed in the first cycle are due to the 1-electron reduction of Mo(V)═O defects present in the catalyst.[14]

The ratio of MoS_x to the VC (Figure S8) support was optimized, and linear sweep voltammetry (LSV) voltamograms of these optimized samples containing 80% active material and 20% VC support are shown in Figure 5a. Electrodes of MoS_6 samples prepared by chemical oxidation with iodine at a mass loading of 1 mg/cm^2 were able to drive current densities of 10 mA/cm^2 (overpotential, η_{10}) at 130 mV, compared to 178 mV for our MoS_4 control samples with a similar mass loading. These samples were also compared to a benchmark Pt catalyst, which required an overpotential of only 44 mV. Stability tests for MoS_6 samples were conducted by running 2000 CV cycles and running an LSV afterward; this LSV (Figure 5b) showed a shift in the η_{10} from 130 to 136 mV suggesting a slight degradation of the catalyst. Experiments carried out in pH 7 phosphate buffer electrolytes showed these materials required higher overpotentials (200 mV) to reach a current density of 10 mA/cm^2 in neutral electrolytes in agreement with previous reports on amorphous molybdenum sulfides (Figure S9).[9] We also investigated the influence of synthetic methods on the activity of catalysts and found that similar overpotentials are found for MoS_6 samples prepared by chemical oxidation with persulfate ($S_2O_8^{2-}$) ion (Figures S10 and S11).

We carried out long-term tests by measuring the currents produced over a 2 h period at a constant potential of 109 mV vs RHE (Figure S12). The currents dropped from an initial value of 5 to ∼4 mA/cm^2. Raman spectroscopy (Figure S13) carried out after long-term tests showed the structures are still made up of Mo_3-like clusters after long-term tests. Further analysis of samples after long-term tests shows a slightly lower S:Mo ratio of ∼5:1 by XPS (Figure S14). Furthermore, we found a change in the ratio of the doublets in the S 2p region. While the initial sample had 58.5% of the sulfur atoms as bridging sulfides, the tested sample showed these bridging sulfides now made up only 33% of sulfur atoms. Similar results have been observed for other a-MoS_x catalysts, and this indicates that bridging sulfides are converted to shared/terminal sulfides in the activation of catalysts; then, during HER catalysis, these terminal sulfides are gradually substituted with water ligands.[24] This gradual loss of terminal sulfur atoms has been shown to be related to the degradation of a-MoS_x catalysts.[18,24]

The overpotentials observed using the sulfur-rich MoS_6 catalyst also compare favorably to MoS_2 and amorphous MoS_x-based materials reported in the literature.[13,25,26] The 5−7 μm thick MoS_3 thin films on FTO (F:SnO_2) substrates reported by Benck et al. achieved similar current densities at an overpotential of 200 mV.[13] Liu et al. similarly showed that 1 μm thick MoS_3 films on FTO substrates required an overpotential of 520 mV while Mo-supported MoS_3 films required 247 mV.[27] More pertinently, a 0.5 mg/cm^2 loading of MoS_3 on multiwalled carbon nanotubes (MWCNTs) achieved a current density of 10 mA/cm^2 at an overpotential of ∼200 mV.[26] Similarly amorphous molybdenum sulfide deposited on graphene liquid crystalline fiber achieved similar current densities at an overpotential of 204 mV.[28]

To investigate if an enhanced surface area was responsible for the improved performance of MoS_6 as a HER catalyst, we carried out electrochemical surface area (ECSA) tests by conducting CV experiments at different scan rates in potential regions where there are no faradaic currents (Figures S15 and 16). The capacitive currents seen here are a function of scan rate (Figure 5c) and represent the double layer capacitance of the materials.[10] MoS_4 has a slightly higher slope at 12.4 mF/cm^2 compared to a slope of 8.9 mF/cm^2 for the MoS_6 sample. This indicates that the MoS_4 sample has a higher surface area, and thus, an enhanced MoS_6 sample surface area is very likely not the reason for the improved performance of the sulfur-rich (MoS_6) catalyst.

As mentioned previously, the MoS_6 catalyst in this report contains relatively more sulfur than other MoS_x catalysts reported in the literature. We anticipate that, like the amorphous ReS_x catalysts mentioned earlier, the primary difference between MoS_6 and other amorphous MoS_2 or MoS_3

DOI: 10.1021/acsaem.8b00973
ACS Appl. Energy Mater. 2018, 1, 4453−4458

catalysts is the presence of more disulfide bonds as either bridging or shared sulfide moieties. Density functional theory (DFT) calculations by Yeo et al. on one-dimensional MoS_x polymers indicate that bridging sulfur (S_2^{2-}) sites have moderately positive Gibbs binding energies for hydrogen adsorption, indicating that these catalysts can optimally adsorb H atoms and desorb H_2 when used as electrodes for the HER.[29] The ratios of the types of sulfur in MoS_2/carbon black (CB) composite catalysts also show similar trends where the activities of catalysts with 6.5% of the total sulfur existing as S_2^{2-} had lower overpotentials for the HER compared to catalysts with only 2% of the sulfur existing as terminal sulfides.[30]

A direct comparison between amorphous MoS_x materials with different S:Mo ratios (MoS_3 and MoS_6) can also be found in the study by Afanasiev et al.,[29] which examined the interactions of both MoS_x species with hydrogen gas. MoS_6 was found to adsorb twice as much hydrogen as MoS_3. The authors attributed this to the possibility that the MoS_6 samples had twice as many of the active sites responsible for S−H_2 interactions.[29] While the adsorbed hydrogen ions (protons) involved in the HER are very different from the H_2 gas used in the studies by Afanasiev et al., the authors show that H_2 is dissociatively adsorbed and likely exists as H−S groups within the solid. We speculate that the same H−S moieties (H adsorbed on terminal sulfur moieties) are involved in the HER, and that the sulfur-rich MoS_6 catalysts have more active sites than the MoS_3 catalysts.[18,29,31] Further work on these catalysts employing in situ EXAFS or in situ Raman spectroscopy will help answer questions about the active sites, intermediates, and mechanism of the HER on sulfur-rich electrocatalysts.

CONCLUSIONS

We have reported a sulfur-rich amorphous MoS_6 HER catalyst for the first time. We used XRD and Raman spectroscopy to show that this MoS_6 catalyst is an amorphous coordination polymer of molybdenum−sulfur (Mo_3S_{13}-like) clusters similar to other amorphous MoS_x catalysts (amorphous MoS_2 and MoS_3), but it likely incorporates the excess sulfur as bridging and terminal sulfide moieties. We plan to confirm the exact structure of the sulfur-rich MoS_x catalyst using advanced techniques like in situ and ex situ extended X-ray absorption fine structure in a future work. When mixed with a Vulcan carbon (VC) support at a mass loading of 1 mg/cm^2, the catalyst is able to drive current densities of 10 mA/cm^2 at an overpotential of 130 mV. This performance is superior to that of our control MoS_4 samples (180 mV) and MoS_3-based catalysts previously reported in the literature, where the overpotentials range from 200 to 250 mV.[13,25−27] We attribute the improved performance of the sulfur-rich MoS_6 to the presence of additional disulfide active sites in this catalyst compared to MoS_2 and MoS_3 electrocatalysts.

ASSOCIATED CONTENT

Supporting Information

The Supporting Information is available free of charge on the ACS Publications website at DOI: 10.1021/acsaem.8b00973.

Detailed experimental information, an XPS survey scan and Mo 3d region scan for the sulfur-rich MoS_6 sample, and DTG and LSV for samples prepared with a persulfate oxidizing agent (PDF)

AUTHOR INFORMATION

Corresponding Author

*E-mail: mullins@che.utexas.edu.

ORCID

Yang Liu: 0000-0002-7240-1546

C. Buddie Mullins: 0000-0003-1030-4801

Notes

The authors declare no competing financial interest.

ACKNOWLEDGMENTS

The authors gratefully acknowledge the National Science Foundation for Grant CHE-1664941 and the Welch Foundation for Grant F-1436. O.M. gratefully acknowledges a National Science Foundation (NSF) Integrative Graduate Education and Research Traineeship (IGERT) Grant 0966298 for financial support. We also acknowledge the National Science Foundation (Grant 0618242) for funding the X-ray photoelectron spectrometer used in this work.

REFERENCES

(1) Bard, A. J.; Fox, M. A. Artificial Photosynthesis: Solar Splitting of Water to Hydrogen and Oxygen Water Splitting. *Acc. Chem. Res.* **1995**, *28*, 141−145.

(2) Lewis, N. S.; Nocera, D. G. Powering the Planet: Chemical Challenges in Solar Energy Utilization. *Proc. Natl. Acad. Sci. U. S. A.* **2006**, *103*, 15729−15735.

(3) Bard, A. J. Inner-Sphere Heterogeneous Electrode Reactions. Electrocatalysis and Photocatalysis: The Challenge. *J. Am. Chem. Soc.* **2010**, *132*, 7559−7567.

(4) Vesborg, P. C. K.; Seger, B.; Chorkendorff, I. Recent Development in Hydrogen Evolution Reaction Catalysts and Their Practical Implementation. *J. Phys. Chem. Lett.* **2015**, *6*, 951−957.

(5) Hinnemann, B.; Moses, P. G.; Bonde, J.; Jørgensen, K. P.; Nielsen, J. H.; Horch, S.; Chorkendorff, I.; Nørskov, J. K. Biomimetic Hydrogen Evolution: MoS_2 Nanoparticles as Catalyst for Hydrogen Evolution. *J. Am. Chem. Soc.* **2005**, *127*, 5308−5309.

(6) Jaramillo, T. F.; Jørgensen, K. P.; Bonde, J.; Nielsen, J. H.; Horch, S.; Chorkendorff, I. Identification of Active Edge Sites for Electrochemical H_2 Evolution from MoS_2 Nanocatalysts. *Science (Washington, DC, U. S.)* **2007**, *317*, 100−102.

(7) McCrory, C. C. L.; Jung, S.; Ferrer, I. M.; Chatman, S. M.; Peters, J. C.; Jaramillo, T. F. Benchmarking Hydrogen Evolving Reaction and Oxygen Evolving Reaction Electrocatalysts for Solar Water Splitting Devices. *J. Am. Chem. Soc.* **2015**, *137*, 4347−4357.

(8) Kibsgaard, J.; Chen, Z.; Reinecke, B. N.; Jaramillo, T. F. Engineering the Surface Structure of MoS_2 to Preferentially Expose Active Edge Sites for Electrocatalysis. *Nat. Mater.* **2012**, *11*, 963−969.

(9) Merki, D.; Fierro, S.; Vrubel, H.; Hu, X. Amorphous Molybdenum Sulfide Films as Catalysts for Electrochemical Hydrogen Production in Water. *Chem. Sci.* **2011**, *2*, 1262−1267.

(10) Merki, D.; Vrubel, H.; Rovelli, L.; Fierro, S.; Hu, X. Fe, Co, and Ni Ions Promote the Catalytic Activity of Amorphous Molybdenum Sulfide Films for Hydrogen Evolution. *Chem. Sci.* **2012**, *3*, 2515−2525.

(11) Morales-Guio, C. G.; Hu, X. Amorphous Molybdenum Sulfides as Hydrogen Evolution Catalysts. *Acc. Chem. Res.* **2014**, *47*, 2671−2681.

(12) Ding, Q.; Song, B.; Xu, P.; Jin, S. Efficient Electrocatalytic and Photoelectrochemical Hydrogen Generation Using MoS_2 and Related Compounds. *Chem.* **2016**, *1*, 699−726.

(13) Benck, J. D.; Chen, Z.; Kuritzky, L. Y.; Forman, A. J.; Jaramillo, T. F. Amorphous Molybdenum Sulfide Catalysts for Electrochemical Hydrogen Production: Insights into the Origin of Their Catalytic Activity. *ACS Catal.* **2012**, *2*, 1916−1923.

(14) Tran, P. D.; Tran, T. V.; Orio, M.; Torelli, S.; Truong, Q. D.; Nayuki, K.; Sasaki, Y.; Chiam, S. Y.; Yi, R.; Honma, I.; Barber, J.;

DOI: 10.1021/acsaem.8b00973
ACS Appl. Energy Mater. 2018, 1, 4453−4458

Artero, V. Coordination Polymer Structure and Revisited Hydrogen Evolution Catalytic Mechanism for Amorphous Molybdenum Sulfide. *Nat. Mater.* **2016**, *15*, 640−646.
(15) Draganjac, M.; Simhon, E.; Chan, L. T.; Kanatzidis, M.; Baenziger, N. C.; Coucouvanis, D. Synthesis, Interconversions, and Structural Characterization of the Molybdenum Sulfide Anions, $[(S_4)_2MoS]^{2-}$, $[(S_4)_2MoO]^{2-}$, $(Mo_2S_{10})^{2-}$ and $(Mo_2S_{12})^{2-}$. *Inorg. Chem.* **1982**, *21*, 3321−3332.
(16) Subrahmanyam, K. S.; Malliakas, C. D.; Sarma, D.; Armatas, G. S.; Wu, J.; Kanatzidis, M. G. Ion-Exchangeable Molybdenum Sulfide Porous Chalcogel: Gas Adsorption and Capture of Iodine and Mercury. *J. Am. Chem. Soc.* **2015**, *137*, 13943−13948.
(17) Afanasiev, P.; Bezverkhy, I. Synthesis of MoS_X (5> X> 6) Amorphous Sulfides and Their Use for Preparation of MoS_2 Monodispersed Microspheres. *Chem. Mater.* **2002**, *14*, 2826−2830.
(18) Ting, L. R. L.; Deng, Y.; Ma, L.; Zhang, Y.-J.; Peterson, A. A.; Yeo, B. S. Catalytic Activities of Sulfur Atoms in Amorphous Molybdenum Sulfide for the Electrochemical Hydrogen Evolution Reaction. *ACS Catal.* **2016**, *6*, 861−867.
(19) Kibsgaard, J.; Jaramillo, T. F.; Besenbacher, F. Building an Appropriate Active-Site Motif into a Hydrogen-Evolution Catalyst with Thiomolybdate $[Mo_3S_{13}]^{2-}$ Clusters. *Nat. Chem.* **2014**, *6*, 248.
(20) Chang, C. H.; Chan, S. S. Infrared and Raman Studies of Amorphous MoS3 and Poorly Crystalline MoS_2. *J. Catal.* **1981**, *72*, 139−148.
(21) Schwarz, D. E.; Frenkel, A. I.; Nuzzo, R. G.; Rauchfuss, T. B.; Vairavamurthy, A. Electrosynthesis of ReS4. XAS Analysis of ReS_2, Re_2S_7, and ReS_4. *Chem. Mater.* **2004**, *16*, 151−158.
(22) Hibble, S. J.; Feaviour, M. R. An in Situ Structural Study of the Thermal Decomposition Reactions of the Ammonium thiomolybdates,$(NH_4)_2Mo_2S_{12}\cdot 2H_2O$ and $(NH_4)_2Mo_3S_{13}\cdot 2H_2O$. *J. Mater. Chem.* **2001**, *11*, 2607−2614.
(23) Huang, Z.; Luo, W.; Ma, L.; Yu, M.; Ren, X.; He, M.; Polen, S.; Click, K.; Garrett, B.; Lu, J.; et al. Dimeric $[Mo_2S_{12}]^{2-}$ Cluster: A Molecular Analogue of MoS_2 Edges for Superior Hydrogen-Evolution Electrocatalysis. *Angew. Chem.* **2015**, *127*, 15396−15400.
(24) Dave, M.; Rajagopal, A.; Damm-Ruttensperger, M.; Schwarz, B.; Nägele, F.; Daccache, L.; Fantauzzi, D.; Jacob, T.; Streb, C. Understanding Homogeneous Hydrogen Evolution Reactivity and Deactivation Pathways of Molecular Molybdenum Sulfide Catalysts. *Sustain. Energy Fuels* **2018**, *2*, 1020−1026.
(25) Huang, H.; Huang, J.; Liu, W.; Fang, Y.; Liu, Y. Ultradispersed and Single-Layered MoS_2 Nanoflakes Strongly Coupled with Graphene: An Optimized Structure with High Kinetics for the Hydrogen Evolution Reaction. *ACS Appl. Mater. Interfaces* **2017**, *9*, 39380−39390.
(26) Lin, T.-W.; Liu, C.-J.; Lin, J.-Y. Facile Synthesis of MoS_3/carbon Nanotube Nanocomposite with High Catalytic Activity toward Hydrogen Evolution Reaction. *Appl. Catal., B* **2013**, *134*−*135*, 75−82.
(27) Liu, B.; Jin, Z.; Bai, L.; Liang, J.; Zhang, Q.; Wang, N.; Liu, C.; Wei, C.; Zhao, Y.; Zhang, X. Molybdenum-Supported Amorphous MoS_3 Catalyst for Efficient Hydrogen Evolution in Solar-Water-Splitting Devices. *J. Mater. Chem. A* **2016**, *4*, 14204−14212.
(28) Lee, K. E.; Sasikala, S. P.; Lee, H. J.; Lee, G. Y.; Koo, S. H.; Yun, T.; Jung, H. J.; Kim, I.; Kim, S. O. Amorphous Molybdenum Sulfide Deposited Graphene Liquid Crystalline Fiber for Hydrogen Evolution Reaction Catalysis. *Part. Part. Syst. Charact.* **2017**, *34*, 1600375.
(29) Afanasiev, P.; Jobic, H.; Lorentz, C.; Leverd, P.; Mastubayashi, N.; Piccolo, L.; Vrinat, M. Low-Temperature Hydrogen Interaction with Amorphous Molybdenum Sulfides MoSx. *J. Phys. Chem. C* **2009**, *113*, 4139−4146.
(30) Xue, N.; Diao, P. Composite of Few-Layered MoS_2 Grown on Carbon Black: Tuning the Ratio of Terminal to Total Sulfur in MoS_2 for Hydrogen Evolution Reaction. *J. Phys. Chem. C* **2017**, *121*, 14413−14425.
(31) Deng, Y.; Ting, L. R. L.; Neo, P. H. L.; Zhang, Y.-J.; Peterson, A. A.; Yeo, B. S. Operando Raman Spectroscopy of Amorphous Molybdenum Sulfide (MoS_x) during the Electrochemical Hydrogen Evolution Reaction: Identification of Sulfur Atoms as Catalytically Active Sites for H^+ Reduction. *ACS Catal.* **2016**, *6*, 7790−7798.

DOI: 10.1021/acsaem.8b00973
ACS Appl. Energy Mater. 2018, 1, 4453−4458